Cooperative polymerization of photosynthetic pigments in formamide-water solution

J. R. E. Fisher, V. Rosenbach-Belkin, and A. Scherz
Department of Biochemistry, The Weizmann Institute of Science, Rehovot 76100, Israel

ABSTRACT The aggregation of bacteriochlorophyll *a* and bacteriopheophytin *a* into large oligomers with maximum optical absorption at 860 nm was studied in a 3:1 (vol/vol) formamide/water solution, using optical absorption spectroscopy and electron microscopy. The aggregation is cooperative and proceeds according to two equilibrium constants. Initially, two pigment molecules form a "seed" that absorbs at ≈860 nm. The equilibrium constant, K_a, governing this reaction equals $1.3 \times 10^3\ M^{-1}$ in the case of bacteriochlorophyll *a* (due to experimental limitations, K_a for bacteriopheophytin *a* could not be determined). The addition of monomers to aggregates consisting of two or more units is governed by an equilibrium constant, K_b, equal to $2.2 \times 10^6\ M^{-1}$ for bacteriochlorophyll *a* and $\approx 10^9\ M^{-1}$ for bacteriopheophytin *a*. The enthalpy and entropy changes that drive the bacteriochlorophyll oligomer formation are −9.25 and ≈0.0 kcal/mol, respectively. Above a threshold concentration, the amount of oligomers remains constant but their length continues to increase. Each oligomer appears to consist of dimers that are associated by hydrophobic interactions among their alcohol residues, forming long strands. Single strands presumably coil into helices that are seen as cylinders. The bacteriochlorophyll *a* oligomers form cylinders with a constant diameter of 150 Å and an average length of 2,000 Å (at 1.5×10^{-5} M bacteriochlorophyll *a*). These cylinders contain 200–250 bacteriochlorophyll *a* dimers. The bacteriopheophytin oligomers coil into wider cylinders (≈400 Å in diameter) which contain ≈600–700 bacteriopheophytin *a* dimers. In both cases, the separation between the dimers is ≈20 Å. At such distances, the dipolar interactions among adjacent dimers are negligible and do not affect the optical absorption of each individual pair. Therefore, the optical absorption of these pairs can be a tool for investigating the absorption pattern of photosynthetic pigments in vivo.

INTRODUCTION

Biological photosynthesis is fueled by solar energy that has been converted into a useful electrochemical potential. This energy conversion results from the joint action of two membrane compartments termed "antennas" and "reaction centers" (RC) (1). The two compartments consist of protein matrices that hold clusters of chlorophylls (Chl), bacteriochlorophylls (Bchl) or other tetrapyrroles (2).

There are profound differences between the spectral properties of the clustered pigments and the isolated monomers in vitro. Most noticable is the in vivo bathochromic shift of the lowest energy (Q_y) transition (1–4). As a result of this shift, the primary electron donor in the RC becomes a kinetic trap which consequently promotes charge separation across the photosynthetic membrane (2).

The origin for the shift of the Q_y transition is still ambiguous. For a long time it was thought to arise from short- and long-range interactions within large oligomers of Chl and Bchl formed in the thylakoid membrane (5–10). The key to the in vivo aggregation of the photosynthetic pigments appeared to be their donor (the lone-pair electrons of the C-9 keto group) and acceptor (unsaturated coordination of the central Mg) properties. This type of dimerization is highly dependent on the extent to which extraneous nucleophiles (e.g., H_2O) compete for coordination with the Mg. Therefore, once it became evident that most of the in vivo Chl and Bchl are hydrogen bonded at their carbonyl functions and strongly ligated at their central Mg to the protein network, this mechanism was no longer tenable (11–18).

Following a different approach, several groups suggested that the pigment's geometry and the bathochromic shift of their Q_y transition are predominantly induced by the surrounding protein whereas the contribution of interactions among the chromophores is minor (16–18). Once the architecture of the bacterial RC was known (12–15), it was argued that these mechanisms for pigment-protein interactions cannot fully account for this bathochromic shift (19–23). On the other hand, the long wavelength–absorbing primary donors, P-860 and P-960, were shown to be tight pairs of Bchl whose centers are separated by 7.0 Å and pyrrole rings overlap (12–15). With this geometry one should expect π–π interactions among the Bchl's ground states and dipolar interactions among their photoexcited states (19–31).

To find the extent to which these interactions determine the pigment geometry and the Q_y shift, Scherz et al.

0006-3495/90/08/461/10 $2.00

studied the formation of small and large aggregates of Chl, Bchl, and their corresponding free bases; pheophytins (Phe) and bacteriopheophytins (Bphe), in mixed solutions of formamide and water (24–28, 30, Scherz, A., and V. Rosenbach-Belkin, submitted for publication). This system was chosen because it imitates the in vivo pigments' environment in two ways; the formamide polymerizes into chains that resemble simple polypeptides (31) and it provides groups for hydrogen bonding with the Bchl molecules. The η transition around 340 nm is evidence that the isocyclic carbonyl oxygen of the Bchl is, indeed, hydrogen bonded to the solvent (29, 32).

While increasing the concentration of Bchl in 3:1 (vol/vol) formamide/water (FW), two spectroscopic forms were observed. One form, termed Bchl-780, had an absorption maximum at ≈780 nm and the other one, termed Bchl-860, had an absorption maximum at ≈860 nm. Above a certain concentration the Bchl-780 remained constant and the Bchl-860 increased linearly (24, 27).

The two forms could be separated by ultracentrifugation or millipore filtration, indicating that Bchl-860 is a large oligomer. The spectra of Bchl-860 and Bchl-780 (after normalization) intersect at three isosbestic points (27), suggesting that, within the concentration range studied, there is a direct conversion from one form to the other. Similar phenomena were observed when other Chl and Bchl were introduced to the FW system. In particular, Bphea, with its maximum absorption at 760 nm (Bphe-760), was completely converted into Bphe-860 even at low concentrations (Scherz, A., and V. Rosenbach-Belkin, submitted for publication, 28). In all the cases mentioned above, the optical absorption of the aggregates closely resembled that of the same pigment in vivo, raising the intriguing possibility that they share a common structural motif (27, 28).

The dependence of [Bchl-780] and [Bchl-860] or [Bphe-760] and [Bphe-860] (the concentrations of the pigment molecules in the corresponding spectroscopic forms) on the total pigment concentration resembles the concentration dependence of monomers and polymers during cooperative polymerization (33). Oosawa and Kasai proposed that two equilibrium constants govern association and dissociation of single monomers from one end of such polymers (33). When the polymer chain is less than a unique seed size, termed s, the addition of monomeric units is governed by K_a, whereas the addition of monomeric units to polymers of length greater than or equal to s is governed by K_b. At equilibrium this phenomenon can be represented by

$$A_n = K_a^{n-1} A_1^n \qquad n < s \tag{1a}$$

$$A_n = K_a^{s-1} K_b^{n-s} A_1^n \qquad n \geq s, \tag{1b}$$

where A_n is the concentration of polymers of length n, A_1 is the monomer concentration, s is the seed size, and $K_a \ll K_b$. In a recent paper Goldstein and Stryer (34) transformed A_n into dimensionless quantities by incorporating the definition $\alpha_n = K_b A_n$ (where K_b was found by Oosawa and Kasai (33) to be the inverse of the asymptotic value of A_1). In doing so, they were able to isolate the components characterizing the system, namely σ and s, where σ was defined as K_a/K_b. In addition, they introduced a new term, ω which was defined as σ^{s-1}. ω represents the cumulative cooperativity collected by the seed (34). Applying these definitions to Eqs. 1a and 1b gives

$$\alpha_n = \sigma^{n-1} \alpha_1^n \qquad n < s \tag{2a}$$

$$\alpha_n = \omega \alpha_1^n \qquad n \geq s \tag{2b}$$

The total concentration of molecules that participate in the process of cooperative polymerization (in units of K_b^{-1}) can be expressed by

$$\alpha_T = \sum_{n=1}^{\infty} n\alpha_n. \tag{3}$$

When Eqs. 2a and 2b are substituted into Eq. 3, α_T becomes

$$\alpha_T = \frac{\alpha_1[1 - s(\sigma\alpha_1)^{s-1}]}{1 - \sigma\alpha_1} + \frac{\alpha_1[\sigma\alpha_1 - (\sigma\alpha_1)^s]}{(1 - \sigma\alpha_1)^2} + \frac{s\sigma^{s-1}\alpha_1^s}{1 - \alpha_1} + \frac{\sigma^{s-1}\alpha_1^{s+1}}{(1 - \alpha_1)^2}. \tag{4}$$

K_a, K_b, and s make a complete set of parameters needed to describe cooperative polymerization. Furthermore, they can be used to define the range of concentrations where the aggregate size is similar to that which is observed in vivo. Studies of the aggregate properties in this concentration range may provide the required information about the contribution of chromophore–chromophore interactions to the spectra and geometry of the in vivo Bchl and other photosynthetic pigments. For this purpose, we set out to derive K_a and s for the Bchl in the FW system (using the value of K_b, calculated directly from the threshold concentration for the formation of large oligomers). In addition, we measured the temperature dependence of K_b to find the driving energy for the pigment association and performed electron microscopy measurements on both Bchl-860 and Bphe-860 to elucidate the structure of the polymers.

MATERIALS AND METHODS

Bchla was extracted and purified from whole cells of *Rhodospirillum rubrum (Rsp. rubrum)* as previously described (24, 26, 27). Sample purity was verified using HPLC (24). Bphea was prepared from Bchla as described (26).

Pigment association or dissociation was monitored by optical and circular dichroism (CD) spectroscopy as described (24). The concentrations of the two spectral forms were calculated from their extinction coefficients; $\epsilon_{780} = 6 \times 10^4\ M^{-1}cm^{-1}$ and $\epsilon_{860} = 1.3 \times 10^5\ M^{-1}cm^{-1}$ for Bchl-780 and Bchl-860, respectively, and $\epsilon_{760} = 5 \times 10^4\ M^{-1}cm^{-1}$ and $\epsilon_{860} = 1.1 \times 10^5\ M^{-1}cm^{-1}$ for Bphe-760 and Bphe-860, respectively (24). The error is within $(1.7 \times 10^{-8} + 1.7 \times 10^{-7} \times OD_{860})$ M for the concentration of Bchl-780 and $(7.7 \times 10^{-9} + 7.7 \times 10^{-8} \times OD_{780})$ M for the concentration of Bchl-860. Similarly, the error is within $(2.0 \times 10^{-8} + 2.0 \times 10^{-7} \times OD_{860})$ M for the concentration of Bphe-780 and $(9.1 \times 10^{-9} + 9.1 \times 10^{-8} \times OD_{760})$ M for the concentration of Bphe-860.

The temperature dependence of Bchl-860 formation was monitored by recording the optical absorption of 1×10^{-6} M Bchla in FW at 20–50°C in ~5°C intervals. At each temperature the sample was equilibrated for ~30 min before the spectrum was recorded.

To perform electron microscopy measurements, a drop of the FW solution containing Bchl-860 (the absorbance [A] at 860 nm was 1.5] or Bphe-860 ($A_{860} = 1.14$), was placed on a parlodion-carbon coated grid (200 mesh) and allowed to adsorb for 1.5 min. Several drops of uranyl acetate (PolyScience Corp., Niles, IL) (0.75% in FW) were added on top of the adsorbant. After 1 min, the remaining stain droplet was removed with filter paper. The sample was dried and examined using a model 410 or 300 electron microscope (Philips Electronic Instruments, Inc., Mahwah, NJ). The solvents used for aggregation (H_2O, formamide (Merck, FRG)) were filtered through 0.45-μm millipore filter.

RESULTS AND DISCUSSION

Fig. 1 shows the optical absorption spectra of Bchl-780, Bchl-860, Bphe-760, and Bphe-860. Fig. 2 describes their concentration dependence where the empty circles represent the concentration of molecules in the bathochromically shifted form and the crosses represent the concentration of the short wavelength–absorbing form.

Apparently, the threshold concentration for the formation of Bchl-860 is 4.55×10^{-7} M $Bchla_T$ (Fig. 2 *a*) and therefore, $K_b = 2.2 \times 10^6\ M^{-1}$. In the case of Bphea, the value of K_b could only be approximated to 10^9 M. Using these values, it was possible to express the concentrations of the two spectral forms for each molecule as dimensionless quantities in terms of α (Fig. 2). To find σ and s, it was first necessary to simplify Eq. 4. It became evident that the equation for α_T reduces to two simple forms under the following conditions. First, when α_1 is smaller than ≈ 0.7 and $\sigma < 10^{-2}$, all the denominators in Eq. 4 are approximately one and the only significant term in all four numerators is the first part of the first term, simply α_1. Thus, when $\alpha_1 < 0.7$, α_T is approximated to

$$\alpha_T \approx \frac{\alpha_1}{1 - \sigma\alpha_1}. \tag{5a}$$

Second, when α_1 approaches one, the denominators in Eq. 4 approach zero. However, since $\sigma \ll 1$ and $(1 - \alpha_i)^2 \ll (1 - \alpha_1)$ for $\alpha_1 \approx 1$, the denominator of the Eq. 4's last term is always much closer to zero than the other three denominators. Therefore, under these conditions the only significant term in Eq. 4 is the last. Thus, when $\alpha_1 \rightarrow 1$, α_T is approximated to

$$\alpha_T \approx \frac{\omega}{[1 - \alpha_1]^2} \tag{5b}$$

When $\alpha_1 = 0$ and $\alpha_1 = 1$ Eqs. 5a and 5b become exact, respectively. Therefore, to find σ and ω we introduced two new terms, $\sigma^* = [(1/\alpha_1) - (1/\alpha_T)]$ and $\omega^* \equiv \alpha_T[1 - \alpha_1]^2$, which can be expanded as polynomial functions of α: $\sigma^* = \Sigma_{i=0} f_i\alpha_1^i$ and $\omega^* = \Sigma_{i=0} g_i\alpha_1^i$, where $f_0 = \sigma$ and $g_0 = \omega$. Plots of the experimentally measured values of σ^* and ω^* for Bchl are shown in Fig. 3, where the solid lines indicate least-squares polynomial fits to the data. The values of σ and ω obtained from these fits are $\sigma = 7 \times 10^{-4}$ and $\omega = 5 \times 10^{-5}$.

Unfortunately, this treatment could not be used for Bphe, because the high value of K_b for the formation of

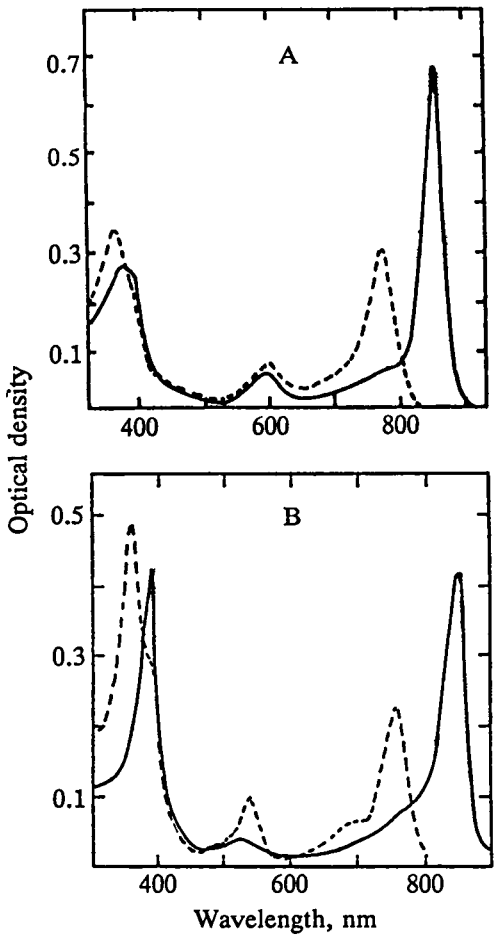

FIGURE 1 (*A*) Absorption of 5.2×10^{-6} M Bchl-860 (——) and 5×10^{-6} M Bchl-780 (---), in FW containing no TX-100 and FW containing 0.125% TX-100, respectively. (*B*) Absorption of 3.7×10^{-6} M Bphe-860 (——) and 3.8×10^{-6} M Bphe-760 (---), in FW containing no TX-100 and 0.125% TX-100, respectively.

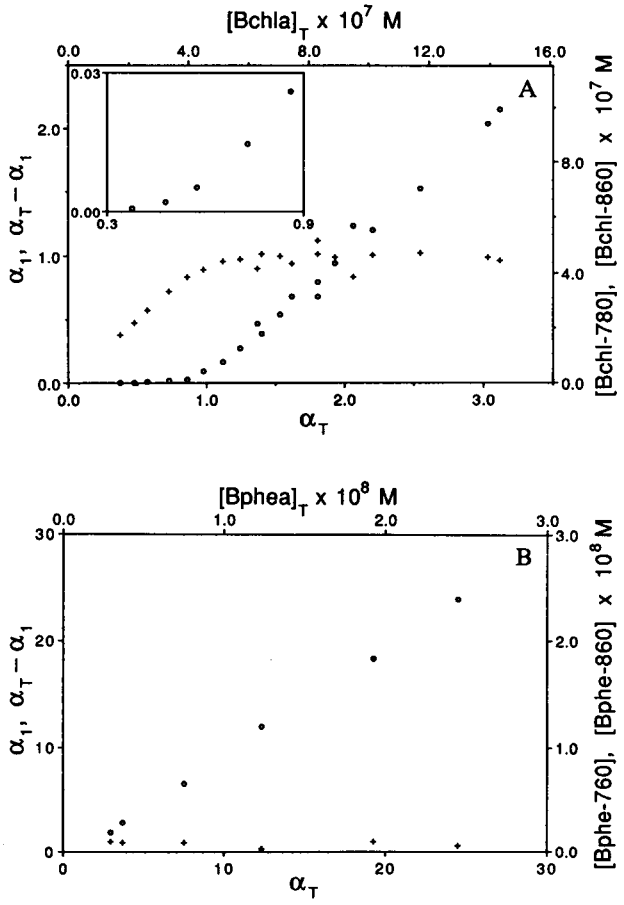

FIGURE 2 (*A*) The dependence of α_1 (+) and $\{\alpha_T - \alpha_1\}$ (○) on α_T for different concentrations of Bchla in FW. The top axis represents the total concentration of Bchla and the right axis represents the concentration of Bchl-780 (+) and Bchl-860 (○). (*B*) The same curves generated for different concentrations of Bphea in FW.

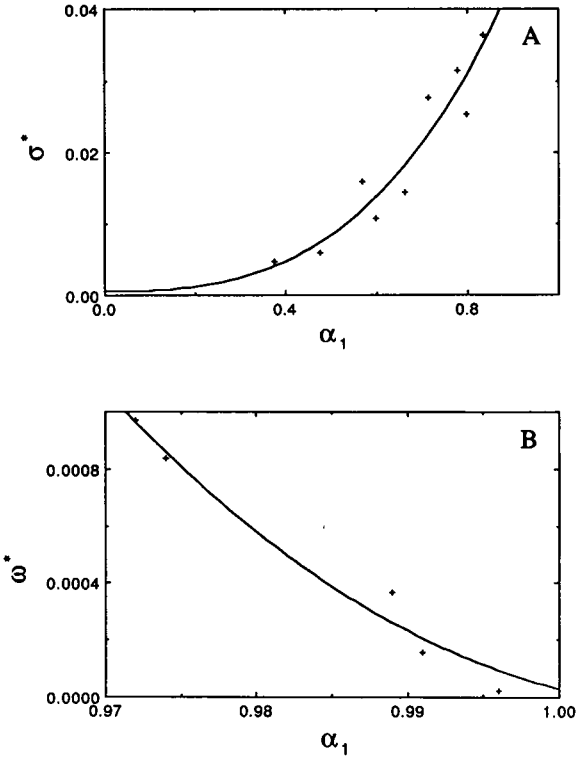

FIGURE 3 (*A*) The dependence of σ^* on α_1 for Bchla, were σ^* is given by Eq. 5a. The solid line describes the best fitting polynomial found by the Macintosh II computer's Cricket Graph Version 1.3 graphics program to be $6.91 \times 10^{-4} - 5.67 \times 10^{-4}\alpha_1 + 5.27 \times 10^{-3}\alpha_1^2 + 5.37 \times 10^{-2}\alpha_1^3$. The correlation between the solid line and the experimental points is 0.973. (*B*). The dependence of ω^* on α_1 for Bchla, where ω^* is given by Eq. 5b. The solid line describes the best fitting polynomial for ω^* (α_1) as $0.74 - 1.47\alpha_1 + 0.73\alpha_1^2$. The correlation between the solid line and the experimental points is 0.989.

Bphe-860 prevented us from monitoring the concentrations of Bphe-760 as α_1 approached zero.[1]

Knowing σ and K_b, K_a was found to equal 1.5×10^3 M^{-1}. And by substituting 5×10^{-5} and 7×10^{-4} for ω and σ, respectively, a value of 2.46 was found for the seed size, s, of Bchla. Since the seed is an integer it must be either 2 or 3.

Substituting these values of K_a, K_b, and s back into Eq. 4 enabled us to express α_1 and $(\alpha_T - \alpha_1)$ in terms of α_T. As exemplified in Fig. 4 *a*, for $K_a = 1.5 \times 10^3$, $K_b = 2.2 \times 10^6$ and $s = 2$ there is a good correlation between the simulated curve and the experimental points. Fig. 4 *c* shows that in order to fit the experimental points given $s = 3$, σ must be ≈ 0.02, however, this is incompatible with our experimental results. As seen in Fig. 3 *a*, σ must be smaller than ≈ 0.005. Therefore, the seed size must be 2.

The theory of cooperative oligomerization (33, 34) predicts that the average aggregation number (the average number of chromophores per oligomer), $\langle i \rangle$, increases abruptly once A_1 approaches K_b^{-1}. Recent theoretical studies predicted that the spectral properties of the Bchla and Bphea large aggregates depend on the aggregation number and the proximity of the individual molecules; namely, if the individual molecules within the aggregate are separated by ≤ 15 Å, an increase of $\langle i \rangle$ from 2 to 50 should increase the bathochromic shift of their Q_y transition by a factor of 2 (35, 36). Using the following equation:

$$\langle i \rangle = \frac{\sum_{n=2}^{\infty} n\alpha_n}{\sum_{n=2}^{\infty} \alpha_n} \qquad (6a)$$

[1]The extrapolation was carried out on the Macintosh II computer using Cricket Graph Version 1.3. Given the following constraints: (*a*) σ must decrease continuously as α_1 decreases and (*b*) ω must decrease continuously as α_1 increases, the program chose polynomials that best fit the experimental values. The correlation between the chosen curves and the experimental points are given in the legend of Fig. 3.

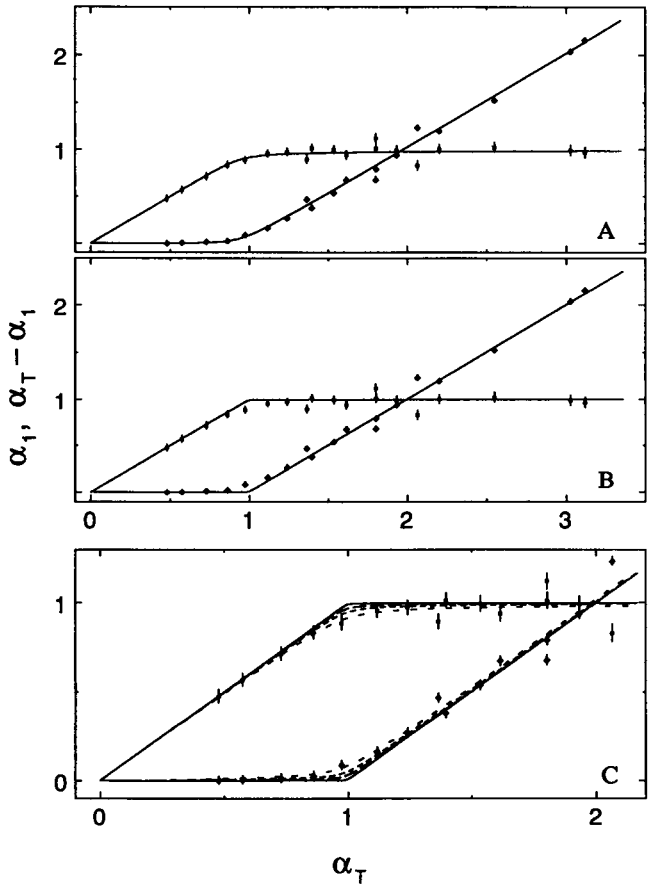

FIGURE 4 The calculated dependence of α_1 and $\alpha_T - \alpha_1$ on α_T using Eq. 4 given: (*A*) $s = 2$, $K = 2.2 \times 10^6$ and $K_a = 1.5 \times 10^3$, (*B*) $s = 3$, $K_b = 2.2 \times 10^6$ and $K_a = 1.5 \times 10^3$, and (*C*) $s = 3$, $K_b = 2.2 \times 10^6$ and $K_a = 1.5 \times 10^3$(———), 1.1×10^4 (——), 2.2×10^4 (- - -), 4.4×10^4 (- -) (the corresponding σ values are 7×10^{-4}, 0.005, 0.01, 0.02). Plots *A*, *B*, and *C* are shown with the experimental points of Fig. 2a and their corresponding error bars.

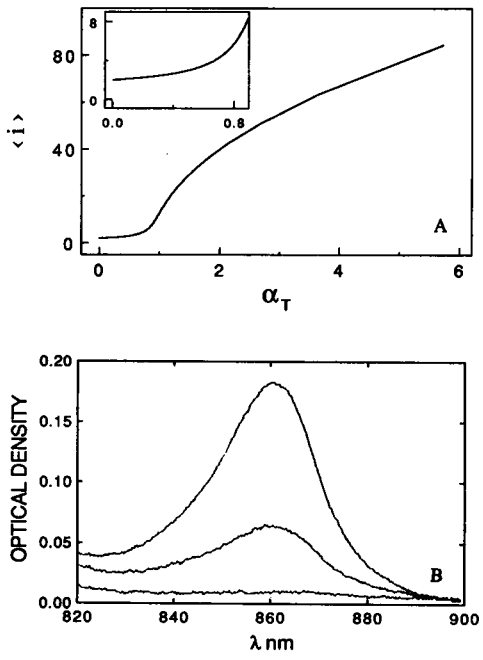

FIGURE 5 (*A*) The dependence of <i> on α_T for $s = 2$ and $\sigma = 7 \times 10^{-4}$ (calculated using Eq. 4 and 6d). (*B*) The optical absorption spectra of Bchl-860 for α_T equals 0.38 (*lower curve*), 0.80 (*middle curve*), and 2.70 (*upper curve*).

where

$$\sum_{n=2}^{\infty} n\alpha_n = \alpha_T - \alpha_1, \tag{6b}$$

and, employing Goldstein and Stryer's formalism for α_n (Eqs. 4 in reference 34) and C_{eq} (Eq. 5 in reference 34), for $s = 2$,

$$\sum_{n=2}^{\infty} \alpha_n = \alpha_2 + C_{eq} = \sigma\alpha_1^2 + \sigma\alpha_1^3\left[\frac{1}{1-\alpha_1}\right], \tag{6c}$$

we found that

$$\langle i \rangle = \frac{(\alpha_T - \alpha_1) \times (1 - \alpha_1)}{\sigma\alpha_1^2}. \tag{6d}$$

A plot of $\langle i \rangle$ vs. α_T for $s = 2$ and $\sigma = 7 \times 10^{-4}$ is shown in Fig. 5 *a*. The optical absorption spectra of three different Bchl concentrations in FW are shown in Fig. 5 *b*. There is a continuous increase of the absorption at ≈858–860 nm as observed in higher concentrations; however, there is no indication of either signal broadening or significant shifting of the maximum absorption wavelength even though the calculated $\langle i \rangle$ values for these solutions increases from ~2 to 50 molecules (Fig. 5 *a*). Therefore, we conclude that the aggregates consist of pigment centers that have a maximum optical absorption at ≈860 nm and are separated by ≥20 Å (center to center). Each pigment center contains not more than two molecules of Bchla because the 860-nm absorption was already observed when $\langle i \rangle \approx 2$. The similarities between the absorption of Bchl-860 and that of Bchla dimers within micelles of Triton X-100 (24, 30), confirms that the pigment centers of the Bchl oligomers are actually made up of two molecules. Because $s = 2$, K_a describes the association of two Bchla monomers, whereas K_b describes the association of two Bchls, one of which is already part of a Bchl oligomer.

The driving forces involved in this type of association were elucidated by examining the temperature dependence of K_b. As the temperature was increased, the threshold concentration of Bchl-780 increased. Because this concentration equals K_b^{-1}, we were able to plot the K_b dependence on 1/T (Fig. 6). From the slope and intercept, we calculated the enthalpy (ΔH) and entropy (ΔS) changes for the large oligomer formation (−9.25 and 0 kcal/mol, respectively).

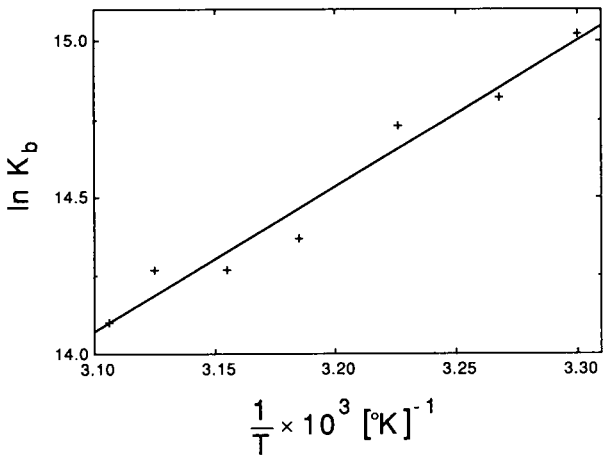

FIGURE 6 The temperature dependence of the second equilibrium constant, K_b, for the Bchl oligomerization in FW. K_b equals the reciprocal of [Bchl-780] at equilibrium for each temperature.

Further information about the supramolecular organization of the Bchla in FW was obtained from the electron microscopy photographs (Fig. 7). Apparently, both the Bchla and Bphea oligomers are large cylinders with virtually constant diameters of 150 and 400 Å, respectively, but in each case the oligomer lengths differ (2,000 Å on the average). It is reasonable to correlate the average cylinder length with the average ⟨i⟩ value. Since the electron microscopy photographs were taken for solutions that contained $\approx 3.3 \times 10^{-5}$ M Bchl, α_T was ≈ 73, α_1 was ≈ 0.997, and ⟨i⟩ was ≈ 320 molecules. This ⟨i⟩ value (calculated by substituting α_T, s, and σ into Eqs. 4 and 6d) should correspond to an average cylinder 150 Å in diameter and 2,000 Å in length. The pigment organization in this cylinder can be speculated considering the following arguments. First, the η transition of Bchl in FW (29, 30) shows that the molecule's C-9 keto group is hydrogen bonded to the solvent and is unable to ligate to the Mg of nearby Bchl. Furthermore, the Q_x transition of the monomeric Bchl (600 nm) indicates that the central Mg is also ligated to the solvent (as in other protic solvents, e.g., methanol). The high concentration of hydrogen donors and nucleophilic agents relative to the pigment concentration prevents the formation of donor-acceptor pairs and enhances the formation of the Bchl π–π or Van der Waals pairs (Fig. 8 *a*) (the geometry of each pair has been described in reference 24). The similar dimerization of the Bphe molecules, where the Mg atom is replaced by two hydrogen atoms, gives further evidence to support our hypothesis. Second, we propose that several pairs form long strands, attaching themselves via hydrophobic interactions among their alcoholic residues (geranylgeraniol for *Rsp. rubrum*) (24) (Fig. 8 *a*). The resulting separation between the Bchl pairs, when considering a maximum overlap of the alcoholic residues, is 20 Å. A similar separation was derived from the simulation of optical absorption and CD spectra (24). It is worthwhile noting that the structure of each strand is reminiscent of the repeating element in the crystals of Chla where such interactions among the alcoholic residues (phytol side chains in Chls) have been assumed (37) (Fig. 8 *b*). Third, to minimize the interactions between the alcoholic residues and the hydrophilic FW environment the strands coil. The observed cylindrical structures are probably helices formed from Bchl polymers in which the hydrophobic tails are separated from the hydrophilic FW by the macrocycle interface. Their formation can account for the giant CD bands observed for Bchl-860 and Bphe-860 in FW (24, 27). Following simple geometrical considerations (Fig. 8 *a*), 20 Bchl pairs are required to produce one turn of a helix whose diameter is 150 Å. The pitch of this helix should be ≈ 200 Å (Fig. 2 *c*). Therefore, the Bchl cylinder (2,000 Å long) should contain 400 molecules of Bchla if one's sole consideration is geometry. This value is quite similar to the calculated ⟨i⟩ value. The Bphe cylinders have a diameter of ≈ 400Å and, therefore, should contain ~600–700 pairs.

The different diameters of the Bchl and Bphe cylinders may be explained by a slightly different geometry of the pigment pairs. The angle between the macrocycle planes that make up the Bchl pair can be smaller than the corresponding angle in the Bphe pair because of a possible interaction between the central Mg of one molecule and the C-2 acetyl of another (24, 39) (in Bphe there is no such interaction because there is no Mg). Therefore, the Bchl pairs are able to form cylinders with a smaller diameter than Bphe.

Upon examining these results more closely, one may suggest that the concentration dependence of Bchl-780 and Bchl-860 is indicative of a different type of micellization, where the alcoholic residues of Bchla point inward and interact hydrophobically, as would other simple amphiphiles that consist of a single hydrocarbon chain with a terminal hydrophilic group. However, several observations reported in this manuscript oppose such a hypothesis. First, the formation of Bchl-860 is exothermic (enthalpy controlled), whereas hydrophobic interactions are usually endothermic (40). Second, the diameter of such micelles should be approximately twice the length of the hydrophobic tail (40) (≈ 20 Å in Bchls and Bphes) but the diameters of the Bchl and Bphe cylinders were 150 Å and 400Å, respectively.

Using small-angle neutron scattering (SANS), Worcester et al. (39) observed similar cylindrical micelles of hydrated Chla, Chlc, Bchla, and pheophytine a (Phea) in aprotic organic solvents. The pigment concentration required for the formation of these micelles was much higher (10^{-2} M) than in the present study ($\leq 10^{-6}$ M) and

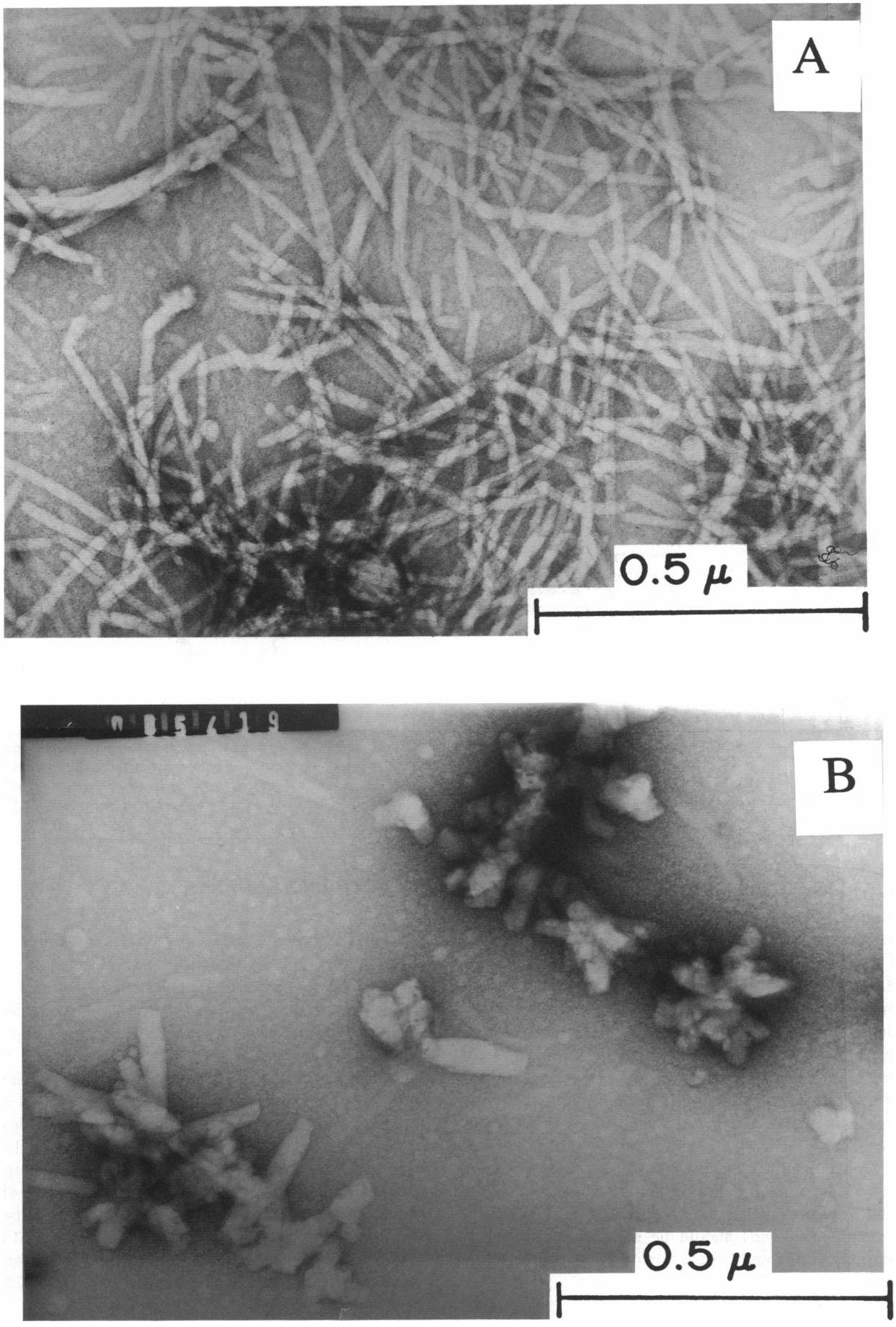

FIGURE 7 (*A*) Electron microscope photograph of Bchla oligomers precipitated by ultracentrifugation from a solution of FW that contained $\approx 10^{-5}$ M Bchla. (*B*) Electron microscope photograph of Bphea oligomers adsorbed on the grid directly from a solution of FW that contained $\approx 10^{-5}$ M Bphea.

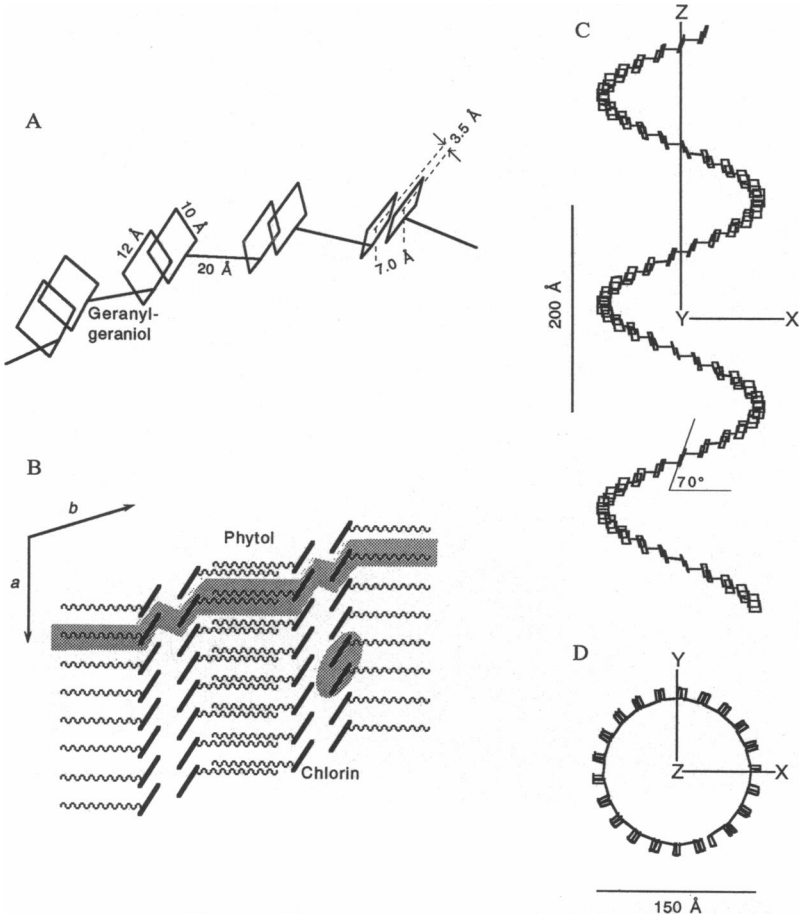

FIGURE 8 (*A*) A section of the proposed structure of the Bchla and Bphea oligomers in FW. Each square represents a pigment molecule and the line connecting two such squares represents two overlapping geranylgeraniols. (*B*) The proposed organization of chlorophyll *a* molecules in crystals (taken from reference 38). Note the similarity between the shaded strand and the strand in *A*. The shaded circle represents two chlorins attached via the central Mg of one and the C-9 keto of the other. (*C*) Side view of several turns of the Bchl helix in FW. (*D*) Top view of one turn of the Bchl helix in FW.

their Bchl Q_y transition was further shifted to the IR (865 nm). The Bchl micelles reported by Worcester et al. (39) contained ≈2 molecules per 100 Å^2. This value is ~20 times the value calculated here, for the Bchl cylinders in FW solution. The discrepancy in the pigment densities and organizations can be explained by different pigment-to-water ratios in the two systems. In the Bchl micelles of Worcester et al. (39) there are ≈6 water molecules per Bchl. This ratio is conducive to bonding of the C-9 keto group of one molecule to the central Mg of another via a single water molecule (Fig. 8 *b*, *stippled circle*). An increase in the relative water concentration (as in the present study) should result in the separation of these adjacent pigment molecules. At the same time, π–π interactions among opposing macrocylces and hydrophobic interactions among the alcoholic residues (Fig. 8 b, *stippled strand*) should be enhanced. Under such conditions, Bchl should aggregate into the proposed single strand.

CONCLUDING REMARKS

The bathochromic shift of the Q_y transition in the pigment centers of antennas and RCs is of primary importance to their function. Attempts to form biomimetic models in which this shift could be varied and studied systematically usually resulted in a complicated mixture of spectral forms that could not add to our understanding. The FW solution, however, was shown to produce homogeneous spectral forms that closely resemble those found in vivo. It was not clear, however, whether the spectral resemblance is accompanied by stoichiometric similarity. We have shown that indeed, the spectral properties of the Bchl oligomers originate from dimers. Therefore, this system can be used to explore the types of chromophore–chromophore interactions that lead to the bathochromic shift of the Bchl special pair's Q_y transition in purple bacteria. For example, the spectra (CD and

optical absorption) of a homogeneous solution of Bchl dimers in vitro reveal excitonic transitions to high-energy states that are usually masked by the accessory Bchl and the Bphe in the RC (Scherz, A., and V. Rosenbach-Blekin, submitted for publication). Furthermore, the self-assembly properties of the Bchl molecules should determine their in vivo geometry and may greatly affect the supramolecular pigment-protein organization (30). These arguments may also be applied to a variety of other photosynthetic pigments that have their Q_y transition shifted during oligmerization in FW (28).

We are grateful to Prof. I. Rubenstein from the Department of Applied Mathematics in the Weizmann Institute of Science for helpful discussions on the cooperative oligomerization formulae. Avigdor Scherz is incumbent of the Recanah Career Development Chair.

This study was financially supported by the United States–Israel Binational Science Foundation (grant No. 84-00144).

Received for publication 4 October 1989 and in final form 9 February 1990.

REFERENCES

1. Okamura, M. Y., G. Feher, and N. Nelson. 1982. Reaction center. *In* Photosynthesis, Energy Conversion by Plants and Bacteria. Govindjee, editor. Academic Press, Inc., New York. 221–227.
2. Zuber, H. 1985. Structure and function of light-harvesting-complexes and their polypeptides. *Photochem. Photobiol.* 42:821–844.
3. Cogdell, R. J., and J. P. Thornber. 1980. Light-harvesting pigment-protein complexes of purple photosynthetic bacteria. *FEBS (Fed. Eur. Biochem. Soc.) Lett.* 122:1–8.
4. Sauer, K., and L. A. Austin. 1978. Bacteriochlorophyll-protein complexes from the light-harvesting antenna of photosynthetic bacteria. *Biochemistry.* 17:2011–2019.
5. Katz, J. J., and K. Ballschmiter. 1968. Wechselwirkungen zwischen chlorophyll and wasser. *Angew. Chem.* 80:283–284.
6. Ballschmiter, K., K. Truesdell, and J. J. Katz. 1969. Aggregation of chlorophyll in nonpolar solvents from molecular weight measurements. *Biochim. Biophys. Acta.* 184:604–613.
7. Ballschmmiter, K., and J. J. Katz. 1972. Chlorophyll-chlorophyll and chlorophyll-water interactions in solid state. *Biochim. Biophys. Acta.* 256:307–327.
8. Katz, J. J. W. Oettmeier, and J. R. Norris. 1976. Organization of antenna and photo-reaction centre chlorophylls on the molecular level. *Phil. Trans. R. Soc. Lond. B.* 273:227–253.
9. Cotton, T. M., P. A. Loach, J. J. Katz, and K. Ballschmiter. 1978. Studies of chlorophyll-chlorophyll and chlorophyll-ligand interactions by visible absorption and infrared spectroscopy at low temperatures. *Photobiol. Photobiol.* 27:735–749.
10. Katz, J. J., L. L. Shipman, T. M. Cotton, and T. R. Janson. 1978. Chlorophyll aggregation: coordination interactions in chlorophyll monomers, dimers and oligomers. *In* The Porphyrins. D. Dolphin, editor. McGraw-Hill Book Co., New York. Vol. V. 401–456.
11. Lutz, M., B. Robert, Q. Zhow, J. M. Newmann, W. Szponarski, and G. Berger. 1988. Protein-prosthetic group interactions in bacterial reaction centers. The photosynthetic bacterial reaction centers, structure and dynamics. *NATO ASI (Adv. Sci. Inst.) Ser. Ser. A Life Sci.* 149:41–50.
12. Deisenhofer, J., O. Epp, K. Miki, R. Huber, and H. Michel. 1985. Structure of the protein subunits in the photosynthetic reaction centre of *Rhodopseudomonas viridas* at 3Å resolution. *Nature (Lond.).* 318:618–624.
13. Chang, H., D. Tiede, J. Tang, U. Smith, J. R. Norris, and M. Schiffer. 1986. Structure of *Rhodopseudomonas sphaeroides* R-26 reaction center. *FEBS (Fed. Eur. Biochem. Soc.) Lett.* 205:82.
14. Allen, J. P., G. Feher, T. O. Yeates, H. Komiya, and D. C. Rees. 1987. Structure of the reaction center form *Rhodobacter sphaeroides* R-26: the cofactors. *Proc. Natl. Acad. Sci. USA.* 84:5730–5734.
15. Allen, J. P., G. Feher, T. O. Yeates, H. Komiya, and D. C. Rees. 1987. Structure of the reaction center from *Rhodobacter sphaeroides* R-26: the protein subunits. *Proc. Natl. Acad. Sci. USA.* 84:6162–6166.
16. Maggiora, L. L. J. D. Petke, D. Gopal, R. T. Iwamoto, and G. M. Maggiora. 1985. Experimental and theoretical studies of Schiff base chlorophylls. *Photochem. Photobiol.* 42:69–75.
17. Eccles, J., and B. Honig. 1983. Charged amino acids as spectroscopic determinants for chlorophyll *in vivo. Proc. Natl. Acad. Sci. USA.* 80:4959–4962.
18. Brunisholz, R. A., and H. Zuber. 1988. Primary structure analyses of bacterial antenna polypeptides. Correlation of aromatic amino acids with spectral properties: structural similarities with reaction center polypeptides. *In* Photosynthetic Light-Harvesting Systems. Organization and Function. H. Scheer, and S. Schneider, editors. Walter de Guyter, Berlin. 103–114.
19. Parson, W. W., A. Warshel, and A. Scherz. 1985. Calculation of the spectroscopic properties of bacterial reaction centers. Antennas and reaction centers of photosynthetic bacteria, structure, interaction and dynamics. *Springer Ser. Chem. Phys.* 42:122–130.
20. Knapp, E. W., P. O. J. Scherer, and S. F. Fischer. 1986. Model studies of low-temperature optical transitions of photosynthetic reaction centers A-, LD-, CD-, ADMR- and LD-ADMR-spectra for *Rhodopseudomonas viridis. Biochim. Biophys. Acta.* 852:295–305.
21. Parson, W. W., and A. Warshel. 1987. Spectoscopic properties of photosynthetic reaction centers. 2. Application of the theory to *Rhodopseudomonas viridis. J. Am. Chem. Soc.* 109:6152–6163.
22. Pearlstein, R. M. 1988. Modified-CI model of protein-induced red shifts of reaction center pigment spectra. The photosynthetic bacterial reaction centers, structure and dynamics. *NATO ASI (Adv. Sci. Inst.) Ser. Ser. A Life Sci.* 149:331–339.
23. Won, Y., and R. A. Friesner. 1988. Temperature dependence of the long wavelength absorption band of the reaction center of *Rhodopseudomonas viridis*. The photosynthetic bacterial reaction centers, structure and dynamics. J. Breton and A. Vermeglio, editors. *NATO ASI (Adv. Sci. Inst.) Ser. Ser. A Life Sci.* 149:341–349.
24. Scherz, A., and V. Rosenbach-Belkin. 1989. Comparative study of optical absorption and circular dichroism of bacteriochlorophyll oligomers in triton X-100, the antenna pigment B850, and the primary donor P-860 of photosynthetic bacteria indicates that all are similar dimers of bacteriochlorophyll a. *Proc. Natl. Acad. Sci. USA.* 86:1505–1509.
25. Scherz, A., V. Rosenbach-Belkin, and J. R. E. Fisher. 1990. Distribution and self-organization of photosynthetic pigments in

micelles: implication for the assembly of light-harvesting complexes and reaction centers in the photosynthetic membrane. *Proc. Natl. Acad. Sci. USA.* In press.

26. Scherz, A., and W. W. Parson. 1984. Oligomers of bacteriochlorophyll and bacteriopheophytin with spectroscopic properties resembling those found in photosynthetic bacteria. *Biochim. Biophys. Acta.* 766:653–665.
27. Scherz, A., V. Rosenbach, and S. Malkin. 1985. Small oligomers of bacteriorchlorophyll as *in vitro* models for the primary electron donors and light-harvesting pigments in purple photosynthetic bacteria: Antennas and reaction centers of photosynthetic bacteria. *Springer Ser. Chem. Phys.* 42:314–323.
28. Scherz, A., and V. Rosenbach-Belkin. 1988. The spectral properties of chlorophyll and bacteriochlorophyll dimers: a comparative study. The photosynthetic bacterial reaction centers, structure and dynamics. *NATO (Adv. Sci. Inst.) Ser. Ser. A Life Sci.* 149:295–308.
29. Rosenbach-Belkin, V. 1988. The primary reactants in bacterial photosynthesis modeling by *in vitro* preparation. Ph.D. thesis. Weizmann Institute of Science, Rehovot, Israel.
30. Scherz, A., V. Rosenbach-Belkin, and J. R. E. Fisher. 1989. Self assembly of bacteriochlorophyll a and bacteriophenophytin a in micellar and non-micellar aqueous solutions: applications to the pigment-protein organization in light-harvesting complexes and reaction centers. *In* Perspectives in Photosynthesis. Proceedings of the 22 Jerusalem Conference in Quantum Chemistry and Biology. J. Jortner and B. Pullman, editors. Kluwer Press, Dodrecht. In press.
31. Hinton, J. F., and R. D. Harpool. 1977. An ab initio investigation of $(formamide)_n$ and $formamide\text{-}(H_2O)_n$ systems. Tentative models for the liquid state and dilute aqueous solution. *J. Am. Chem. Soc.* 99:349–333.
32. Renge, I., and R. Avarmaa. 1985. Specific solvation of chlorophyll a: solvent nucleophility, hydrogen bonding and steric effects on absorption spectra. *Photochem. Photobiol.* 42:253–260.
33. Oosawa, F., and M. Kasai. 1962. A theory of linear and helical aggregations of macromolecules. *J. Mol. Biol.* 4:10–21.
34. Goldstein, R. F., and L. Stryer. 1966. Cooperative polymerization reactions analytical approximations, numerical examples, and experimental strategy. *Biophys. J.* 50:583–599.
35. Lalonde, D. E., J. D. Petke, and G. M. Maggiora. 1989. Evaluation of approximations in molecular exciton theory. 2. Application to oligometric systems of interest in photosynthesis. *J. Phys. Chem.* 93:608–614.
36. Parson, W. W., S. Creighton, and A. Warshel. 1989. Calculations of charge-transfer transition energies and spectroscopic properties of a molecular crystal: methylbacteriopheophorbide a. *J. Am. Chem. Soc.* 111:4277–4284.
37. Kratky, C., and J.D. Dunitz. 1977. Ordered aggregation states of chlorophyll a and some derivatives. *J. Mol. Biol.* 113:431–442.
38. Katz, J. J., H. H. Strain, A. L. Harkness, M. H. Studier, W. A. Svec, T. R. Janson, and B. T. Cope. 1972. Esterfying alcohols in the chlorophylls of purple photosynthetic bacteria. A new chlorophyll, bacteriochloropyll (gg), *all-trans*-geranylgeranyl bacteriochlorophyllide a. *J. Am. Chem. Soc.* 94:7938–7939.
39. Worcester, D. L., T. J. Michalski, and J. J. Katz. 1986. Small-angle neutron scattering studies of chlorophyll micelles: models for bacterial antenna chlorophyll. *Proc. Natl. Acad. Sci. U.S.A.* 83:3791–3795.
40. Tanford, C. 1980. The hydrophobic effect: formation of micelles and biological membranes. John Wiley & Sons, Inc., New York, 233 pp.